Tangent and cotangent states of the electromagnetic field

John J. Slosser

Department of Physics, University of Arizona, Tucson, Arizona 85721

Pierre Meystre

Optical Sciences Center, University of Arizona, Tucson, Arizona 85721
(Received 25 August 1989)

We consider a lossless micromaser in which a monoenergetic, low-density beam of two-level atoms in a coherent superposition of their upper and lower states is injected inside a single-mode high-Q cavity. This is a realization of a harmonic oscillator driven by a quantum current. We find that under appropriate conditions the field may evolve to pure states, which we call tangent and cotangent states, even for mixed-state initial conditions. In various limits, they exhibit nonclassical properties such as sub-Poissonian photon statistics, or even more interestingly acquire the characteristics of "macroscopic" quantum superpositions. The conditions under which these states are reached, as well as the dynamical approach of the system to steady state, are discussed in detail.

I. INTRODUCTION

The last few years have witnessed considerable activity towards the generation and detection of nonclassical states of the electromagnetic field. Squeezed and sub-Poissonian fields have recently been produced.[1] There is also good reason to believe that number states of the electromagnetic field will be generated in the near future, a promising scheme involving a micromaser with negligible cavity losses. Filipowicz, Javanainen, and Meystre[2] have shown that if inverted atoms with a well-defined velocity are injected inside a micromaser cavity, it is possible for the field to evolve towards a number state $|n\rangle$.

The present paper further studies the generation of nonclassical fields in a micromaser. It extends and generalizes our previous results to the case where the two-level atoms are injected inside the cavity in a coherent superposition of their upper and lower states.[3] We find that the field may evolve to pure states of the field even for mixed-state initial conditions. We call these new states tangent and cotangent states of the harmonic oscillator. In various limits, they exhibit nonclassical properties such as sub-Poissonian photon statistics, or even more interestingly acquire the characteristics of "macroscopic" quantum superpositions.

As pointed out by Cummings and Rajagopal,[4] such results might seem surprising at first: it is a common perception that when the density matrix is reduced (the atomic variables traced out) after successive atoms exit the cavity, information is discarded. Thus the entropy of the field mode would be expected to increase. Rather, while computing this entropy for a micromaser pumped by inverted atoms under conditions such that it evolves to a number state,[2] they found that after an initial increase, it eventually decreases to zero.[4] We find that a similar decrease of the entropy can occur for a cavity pumped by a coherent superposition of their upper and lower states, a signature that the maser mode evolves to a pure state.

This paper is organized as follows. Section II describes our model and presents selected results from numerical experiments showing the evolution of the cavity mode to a pure state of the field. These results show a large variety of possible steady states, some sub-Poissonian and some with the character of "macroscopic" quantum superpositions. Section III derives the mathematical form of these states from a general factorization argument, and uses boundary conditions to select between tangent and cotangent states for given initial conditions. Section IV uses a simple graphical construction to determine general properties of the cotangent states. In particular, this permits us to predict under which conditions cotangent states acquire the character of "macroscopic" superpositions, become sub-Poissonian, or approach the properties of coherent states. Section V turns to an eigenvalue analysis of the micromaser map. We introduce a space of "supervectors" that describes all physically meaningful density matrices, reduce the micromaser return map to this space, and find the eigenvectors with unit eigenvalue corresponding to steady states of the system. We further demonstrate the possibility of "period-2" oscillations in the cavity mode dynamics. Finally, Section VI is a summary and conclusion.

II. NUMERICAL RESULTS

We consider a micromaser[5] in which a monoenergetic, low-density beam of two-level atoms is injected inside a single-mode, high-Q cavity. The injection rate is low enough that at most one atom at a time is present inside the resonator, but still high enough that a large number of atoms can be injected before cavity damping becomes important. Under these conditions, the dynamics of the system is obtained by successive applications of the Jaynes-Cummings evolution operator.[6] We assume that the field is described by the density matrix ρ_0 at the instant when the first atom enters the cavity in a state described by the density matrix $\rho_a(0)$. After the interaction

time τ, the field density matrix reduces to

$$\rho_1(\tau)=\mathrm{Tr}_a[U(\tau)\rho_0\rho_a U^\dagger(\tau)] \ , \tag{2.1}$$

where the trace is over the atomic variables. Here $U(\tau)$ is the interaction picture Jaynes-Cummings evolution operator $U(\tau)=\exp(-iV\tau/\hbar)$, and the Jaynes-Cummings Hamiltonian is $H=H_0+V$ with

$$H_0=\hbar\omega a^\dagger a+\hbar\omega\sigma_z \ , \tag{2.2a}$$

$$V=\hbar\kappa(a\sigma_+ +a^\dagger\sigma_-) \ . \tag{2.2b}$$

The field mode creation and annihilation operators $a^\dagger$ and a obey the commutation relation $[a,a^\dagger]=1,\sigma_z,\sigma_+$, and σ_- are Pauli spin matrices and κ is the atom-field dipole coupling constant. We assume exact resonance between the field frequency and the atomic transition frequency, and in writing Eq. (2.1) we have assumed that the state of the atom is not measured as it exits the cavity. Hence the corresponding trace operation is sometimes referred to as a nonselective measurement.[7]

In the interaction picture and in the absence of dissipation, the field density matrix does not evolve during the interval T between atoms. Thus successive iterations yield the field density matrix after l atoms as

$$\rho_l=\mathrm{Tr}_a[U(\tau)\rho_{l-1}\rho_a U^\dagger(\tau)]=\mathrm{Tr}_a(U(\tau)\rho_a\mathrm{Tr}_a\{U(\tau)\rho_a\cdots[U(\tau)\rho_a\rho_0 U^\dagger(\tau)]\cdots U^\dagger(\tau)\}U^\dagger(\tau)) \ . \tag{2.3}$$

While numerically solving Eq. (2.3) for the initial atomic density matrix

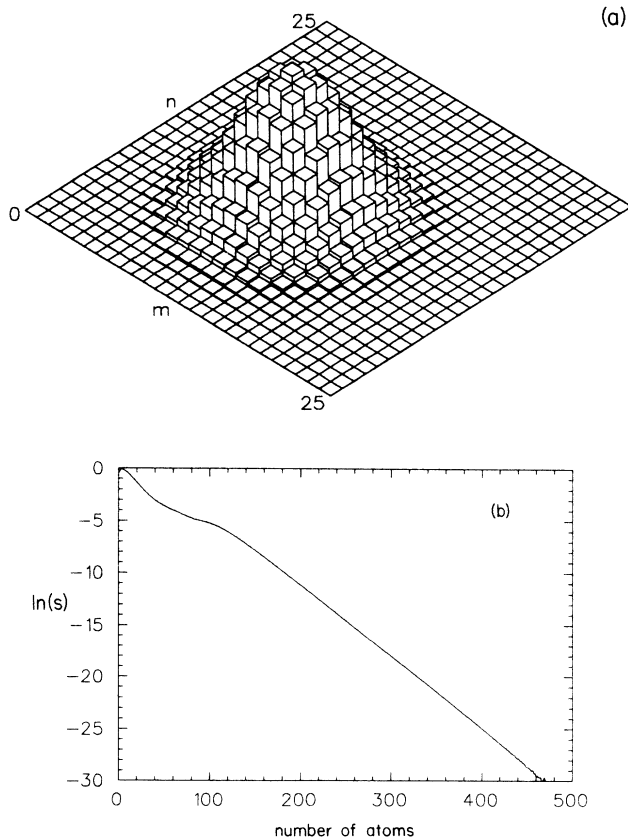$$\rho_a=(\alpha|a\rangle+\beta|b\rangle)(\alpha^*\langle a|+\beta^*\langle b|) \tag{2.4}$$

FIG. 1. (a) Moduli of the steady-state density-matrix elements $\rho_{nm}=\langle n|\rho|m\rangle$ of the pure state reached by the harmonic oscillator driven by a steam of spin-$\frac{1}{2}$ particles in a coherent superposition of upper and lower states. The upper state population is $|\alpha|^2=0.75$, and the Fock state $|25\rangle$ is a π-trapping state $\sqrt{26}\kappa\tau=\pi$. The field mode was started from a thermal state with mean excitation $\langle n\rangle=10^{-1}$. The initial distribution has been slightly truncated and renormalized to avoid any initial population past the state $|25\rangle$. (b) Entropy of the harmonic oscillator (on a ln scale) as a function of the number of spins having interacted with it.
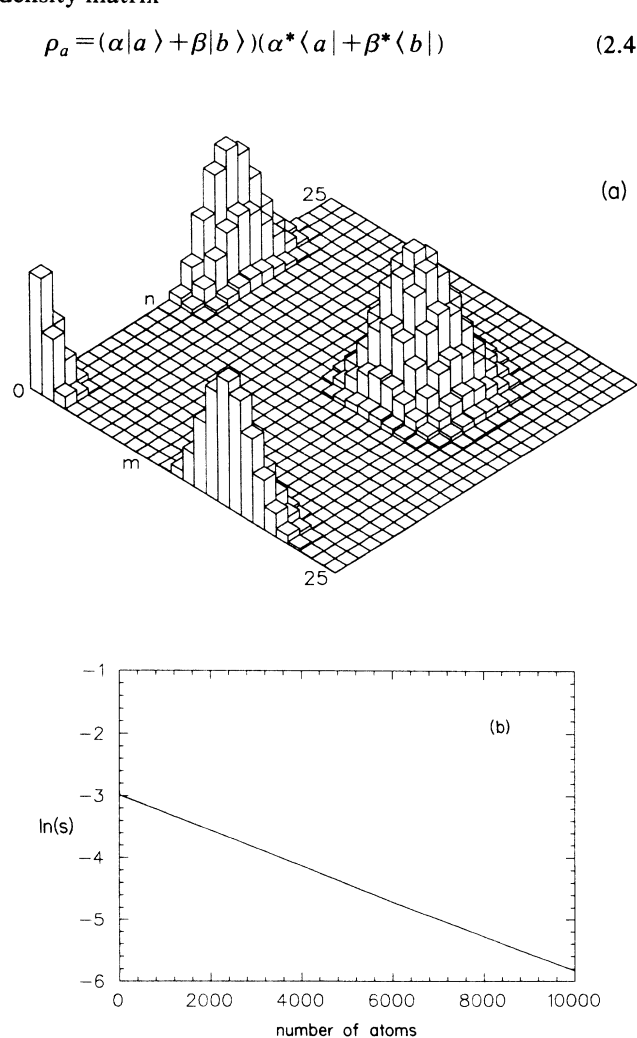

FIG. 2. Same as Fig. 1, but with the Fock state $|25\rangle$ being now a 3π-trapping state $\sqrt{26}\kappa\tau=3\pi$ and $|\alpha|^2=0.39$. In this case, the field mode evolves toward a pure state that resembles a "macroscopic superposition."

with $|\alpha|^2+|\beta|^2=1$, $|a\rangle$ and $|b\rangle$ being the upper and lower atomic states, we found that the reduced density matrix for the oscillator alone can evolve towards a pure (zero-entropy) steady state, provided that a number of conditions are met. These conditions will be specified precisely in Sec. III. For now, it suffices to mention that they include the "trapping condition"[2]

$$(N+1)^{1/2}\kappa\tau=q\pi \quad (N,q \text{ integers}) , \quad (2.5)$$

for the spin-field interaction strength $\kappa\tau$, as well as the fact that density matrix must be such that the probability of finding n photons initially in the cavity is zero for $n > N$. Examples of final states reached by the harmonic oscillator under such conditions are given in Figs. 1 and 2. Figure 1(a) gives the modulus of the density matrix elements $\rho_{n,m}=\langle n|\rho|m\rangle$ of the final state reached by a cavity mode initially in a (truncated) thermal mixture with an average photon number $\langle n\rangle=10^{-1}$. In this example the number state $|25\rangle$ is a "π-trapping state" $\sqrt{26}\kappa\tau=\pi$, and the truncation is such that there is no initial population past this state. The evolution of the field entropy $S_l=-k_B\mathrm{Tr}\rho_l\ln\rho_l$, where k_B is Boltzmann's constant, as successive atoms are passed through the cavity is given in Fig. 1(b). After an initial transient, S_l decreases monotonically and eventually decays exponentially to zero, indicating that the asymptotic state of the field is a pure state. This exponential decay is further discussed in Sec. V in terms of the eigenvalues of the micromaser return map.

Figure 2 gives similar results, except that the state $|25\rangle$ is now a "3π-trapping state" $\sqrt{26}\kappa\tau=3\pi$. Again, the evolution of the field entropy indicates that the system evolves to a pure state. Note however the qualitative difference between the single-peaked final state for a π trap and the double-peaked photon statistics ρ_{nn} corresponding to the 3π-trap situation. Note also the much slower approach to steady state in this last case. As shown in Sec. III, the state of Fig. 1 is sub-Poissonian, while that of Fig. 2 is clearly super-Poissonian.

A state with photon statistics similar to that of Fig. 2(a) is illustrated in Fig. 3. However, the nonzero final entropy indicates that the field evolves now to a mixed state. This is seen even more clearly in the considerable
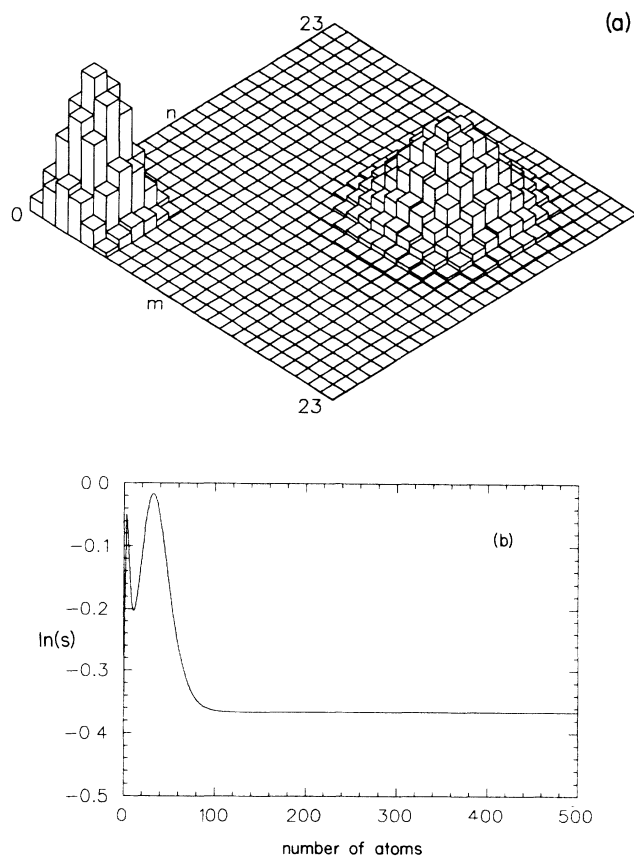

FIG. 3. Same as Fig. 1, but the field evolution is bound by the 2π trap $|N\rangle=|23\rangle$, i.e., $\sqrt{24}\kappa\tau=2\pi$. Note that under this condition the number state $|5\rangle$ is a π-trapping state $\sqrt{6}\kappa\tau=\pi$ so that the initial field photon statistics spans two disconnected regions of Fock space. In this case, the field mode evolves to a mixed state, as further illustrated by the field entropy.
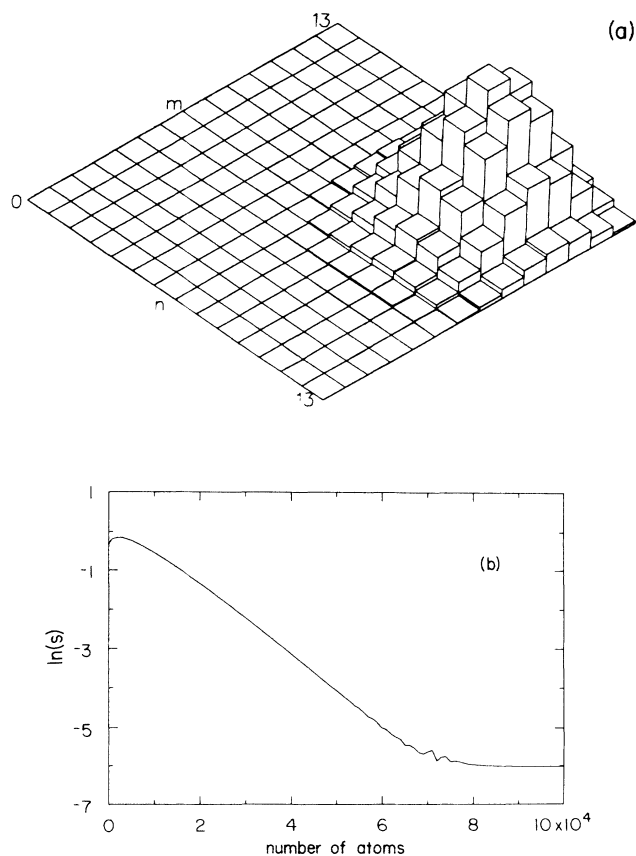
FIG. 4. Same as Fig. 1, but with the number state $|13\rangle$ being now a 2π trap $\sqrt{14}\kappa\tau=2\pi$ and $|\alpha|^2=0.85$. Although there is no accidental trap between the vacuum state and this trap in this case, the field still evolves toward a mixed state.

reduction of the off-diagonal density-matrix elements $\rho_{n,m}$ as compared to the situation of Fig. 2(a). In this example, we have taken the number state $|23\rangle$ to be a 2π-trapping state $\sqrt{24}\kappa\tau=2\pi$, hence the number state $|5\rangle$ is a π-trapping state $\sqrt{6}\kappa\tau=\pi$. We show in Sec. III that the trapping states (2.5) divide the Fock space of the cavity mode into disconnected regions: the dipole interaction (2.2) does not couple density-matrix elements between these regions. Hence, no coherences can be generated between number states below and above the number state $|6\rangle$. In the example of Fig. 3, the states $|n\rangle$ with $n>6$ of the initial thermal field are significantly populated, hence the micromaser field must remain mixed under the Jaynes-Cummings dynamics.

Figure 4 shows another situation leading to a mixed final state of the field. Here, the number state $|13\rangle$ is a 2π-trapping state $\sqrt{14}\kappa\tau=2\pi$. After a rapid initial decay, the field entropy remains constant and larger than zero.

These numerical examples illustrate several important features of the dynamics of the micromaser field. First, the trapping states (2.5) lead to the existence of normalizable steady states of the field in the absence of cavity losses, even for initially inverted atoms. Second, the nature of the final states depends strongly on the "parity" of the trapping states by which they are bounded, where by parity we mean the odd or even parity of q in Eq. (2.5).

We show in Sec. III that if there are no accidental intervening traps between these bounds, then the evolution of the field is towards pure states if it is bounded by traps of opposite parities, and is towards mixtures for traps of same parity. In the presence of intervening traps, the system dynamics can become quite complex, involving, e.g., period-2 oscillations under appropriate conditions.

The evolution of the field towards pure states is a surprising result at first: In general, partial traces such as those that appear in Eq. (1) are expected to lead to mixtures, although exceptions do exist, e.g., the classically driven damped oscillator at zero temperature.[8] What happens in the present case is that the harmonic oscillator appears to benefit from a transfer of coherence from the spins. Sections III–V determine the general properties of these new states and show that in various limits they acquire nonclassical properties such as sub-Poissonian statistics, or more interestingly resemble "macroscopic" superpositions. As such they may provide new testing grounds for fundamental tests of quantum mechanics and measurement theory.

III. TANGENT AND COTANGENT STATES

Under the Jaynes-Cummings dynamics, the evolution of an arbitrary state of the oscillator–two-level-atom coupled system is given in the interaction picture by[6]

$$\sum_n s_n|n\rangle(\alpha|a\rangle+\beta|b\rangle)\rightarrow\sum_n s_n[\alpha\cos(\sqrt{n+1}\kappa\tau)|n\rangle+i\beta\sin(\sqrt{n}\,\kappa\tau)|n-1\rangle]|a\rangle$$

$$+\sum_n s_n[\beta\cos(\sqrt{n}\,\kappa\tau)|n\rangle+i\alpha\sin(\sqrt{n+1}\kappa\tau)|n+1\rangle]|b\rangle\equiv|f_a\rangle|a\rangle+|f_b\rangle|b\rangle. \qquad (3.1)$$

The existence of trapping states is immediately apparent from this equation: if for some $n=N$ we have

$$\sqrt{N}\,\kappa\tau=q\pi, \quad q \text{ integer}, \qquad (3.2)$$

then the downward coupling between $|N\rangle$ and $|N-1\rangle$ vanishes and the regions of Fock space below and above $|N\rangle$ are dynamically disconnected. We call $|N\rangle$ a downward $q\pi$-trapping state. Similarly, a state such that

$$\sqrt{N+1}\kappa\tau=q\pi, \quad q \text{ integer} \qquad (3.3)$$

is an upward $q\pi$-trapping state. Equations (3.2) and (3.3) show that the state immediately following an upward $q\pi$-trapping state is always a downward $q\pi$-trapping state. Since trapping states separate the Fock space of the oscillator into disconnected blocks, initial conditions within one block cannot leak into others. This is the essential ingredient leading to the existence of normalizable steady states of the harmonic oscillator in the absence of dissipation. Filipowicz, Javanainen, and Meystre[2] showed how to exploit these states to generate number states of the electromagnetic field by injecting inverted atoms inside a single-mode cavity. This section generalizes these results to the case where atoms in a coherent superposition of upper and lower states are utilized.[3]

Since the driven oscillator's dynamics can be handled

separately in disconnected regions of Fock space we concentrate on initial conditions within one such region only. Under more general initial conditions the harmonic oscillator always evolves towards a mixed state, since the dynamics prohibits the build up of coherences between disconnected blocks, see Fig. 3.

Guided by the numerical results of Sec. II, we develop a self-consistency argument to determine the pure steady state reached by the field mode. We assume that the field is in the pure state

$$|f\rangle=\sum_{n=N_d}^{N_u} s_n|n\rangle \qquad (3.4)$$

after interaction with a given atoms, where the number states $|N_d\rangle$ and $|N_u\rangle$ are the lower and upper boundaries of the Fock space block under consideration. Requiring that it remains in this same state (within an overall phase) after interaction with the next atom imposes that the state of the composite system at time τ factorizes into a tensor product of a field state $|f\rangle$ times a pure state of the two-level atom,

$$|f\rangle(\alpha|a\rangle+\beta|b\rangle)\rightarrow e^{i\phi}|f\rangle(\alpha'|a\rangle+\beta'|b\rangle). \qquad (3.5)$$

Here $|\alpha'|^2+|\beta'|^2=1$ and α',β' as well as the overall phase ϕ are independent of n. Comparing Eqs. (3.5) and (3.1)

gives readily

$$\alpha' e^{i\phi} |f\rangle = |f_a\rangle , \tag{3.6}$$

$$\beta' e^{i\phi} |f\rangle = |f_b\rangle . \tag{3.7}$$

With the definitions (3.1) of $|f_a\rangle$ and $|f_b\rangle$, these two equations yield the recurrence relations

$$s_n = \frac{i\beta \sin(\sqrt{n+1}\kappa\tau)}{\alpha' \exp(i\phi) - \alpha \cos(\sqrt{n+1}\kappa\tau)} s_{n+1} , \tag{3.8}$$

$$s_n = -i \frac{\beta' \exp(i\phi) - \beta \cos(\sqrt{n+1}\kappa\tau)}{\alpha \sin(\sqrt{n+1}\kappa\tau)} s_{n+1} , \tag{3.9}$$

which must be satisfied simultaneously for all n's within the Fock space block under consideration. These conditions are satisfied under the two possible conditions

$$\alpha\beta' = -\alpha'\beta , \tag{3.10}$$

$$\alpha\beta = -\alpha'\beta' e^{2i\phi} . \tag{3.11}$$

Assuming without loss of generality that α, β, α', and β' are real we find

$$e^{i\phi} = \pm 1, \quad \alpha' = \mp\alpha, \quad \beta' = \pm\beta \tag{3.12}$$

or

$$e^{i\phi} = \pm 1, \quad \alpha' = \pm\alpha, \quad \beta' = \mp\beta . \tag{3.13}$$

No other zero-entropy steady states are possible under the Jaynes-Cummings dynamics. Setting $\exp(i\phi) = 1$ without loss of generality, Eq. (3.12) can be interpreted as a nutation of the upper-state probability amplitude by π and Eq. (3.13) as a nutation of the lower-state probability amplitude by π. Equations (3.12) and (3.13) yield simple recurrence relations for the probability amplitudes s_n of Eq. (3.4). We find readily

$$s_n = i(\alpha/\beta)\cot(\sqrt{n}\,\kappa\tau/2)s_{n-1} \tag{3.14}$$

in the first case and

$$s_n = -i(\alpha/\beta)\tan(\sqrt{n}\,\kappa\tau/2)s_{n-1} \tag{3.15}$$

in the second case. The corresponding photon statistics are

$$|s_n|^2 = |\alpha/\beta|^2\cot^2(\sqrt{n}\,\kappa\tau/2)|s_{n-1}|^2 , \tag{3.16}$$

$$|s_n|^2 = |\alpha/\beta|^2\tan^2(\sqrt{n}\,\kappa\tau/2)|s_{n-1}|^2 \tag{3.17}$$

For this reason we call these states cotangent and tangent states of the harmonic oscillator, respectively.

We still need to verify that the states (3.14) and (3.15) satisfy the trapping condition (3.3) at the boundaries of the phase-space block under consideration. The Appendix shows that these boundary conditions are satisfied provided that the upper and lower trapping states $|N_u\rangle$ and $|N_d\rangle$ have opposite parities: specifically, the cotangent state (3.14) only satisfies the boundary conditions if $\sqrt{N_d+1}\kappa\tau = q\pi$, q even and $\sqrt{N_u+1}\kappa\tau = p\pi$, p odd. The reverse is true for the tangent solution (3.15): in that case q must be odd and p even. Note that since typical initial conditions include a finite population of the vacu-

um state, cotangent states are physically more relevant than tangent states. We concentrate primarily on the properties of cotangent states in the following.

IV. BASIC PROPERTIES

In this section we use a simple argument to determine the general properties of the cotangent states. In particular, we predict under which conditions they acquire the character of "macroscopic" superpositions, become sub-Poissonian, or approach the properties of coherent states. We concentrate for concreteness on cotangent states which include the vacuum state $|N_d\rangle = |0\rangle$. Our discussion can be generalized to other situations straightforwardly. We proceed by noting that the recurrence relation (3.14) indicates that $|s_n| > |s_{n-1}|$ provided that

$$\cot(\sqrt{n}\,\kappa\tau/2) > \beta/\alpha . \tag{4.1}$$

The cotangent function $\cot(x)$ is illustrated in Fig. 5, where we have also drawn a horizontal line at β/α. We should keep in mind that for a given interaction strength $\kappa\tau$, only the discrete set of arguments x such that

$$4x^2/\kappa^2\tau^2 = n, \quad n \text{ integer} \tag{4.2}$$

are physically meaningful.

From the discussion of the preceding section, we know that the existence of cotangent states requires that condition (4.2) be satisfied at $x = (2q+1)\pi/2$ with q being an integer. Consider first the simplest case $q = 1$, where the cotangent state is terminated at a π trap. If the first value of x such that (4.2) is satisfied $x = \sqrt{1}\kappa\tau/2$ is also such that $\cot(x) < \beta/\alpha$, then from Eq. (4.1) we have that $s_1 < s_0$ and the cotangent state is peaked at $n = 0$. In contrast, if this point is such that $\cot(x) > \beta/\alpha$, then $s_1 > s_0$. In this case, the photon statistics are not peaked at $n = 0$, but rather at the last number state $|n\rangle$ such that Eq. (4.1) is satisfied and such that $0 \le x \le \pi/2$ satisfies Eq. (2.4).

Figure 6 gives the mean photon number and the normalized second moment $\sigma = (\langle n^2\rangle - \langle n\rangle^2)/\langle n\rangle$ as a
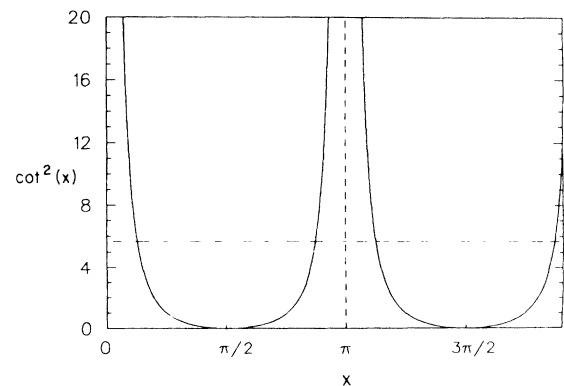
FIG. 5. $\cot^2(x)$ function and horizontal line at β/α used in the graphic determination of the photon statistics of the cotangent state.
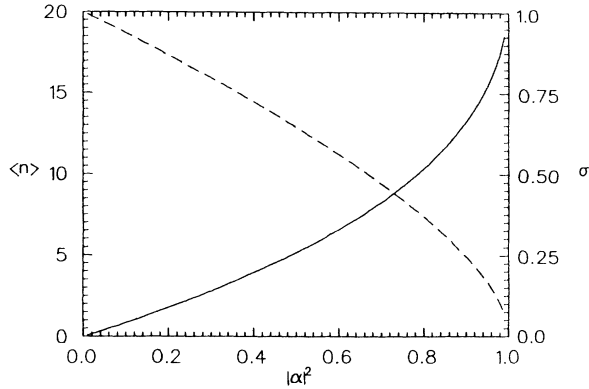
FIG. 6. Mean photon number (solid line) and normalized standard deviation (dashed line) of a cotangent state bound between the vacuum and the π trap $|21\rangle$ as a function of the upper-state population $|\alpha|^2$.

function of α for cotangent states bound between the vacuum state and a π trap $|N_1\rangle$. For fully inverted spins ($\alpha = 1$) the system evolves precisely towards the Fock state $|N_1\rangle$. For $\alpha = 0$, in contrast, it asymptotically reaches the vacuum state $|0\rangle$. For intermediate situations, the resulting cotangent state is sub-Poissonian.

Although cotangent states bound between the vacuum and a π-trapping state $|N_1\rangle$ are sub-Poissonian, Fig. 1 shows that their photon statistics resemble those of a coherent state. For cotangent states such that significant populations are limited to number states $|n\rangle$ such that $\kappa\tau \ll 1/\sqrt{n}$ we have

$$|s_n|^2 \simeq |2\alpha/\beta\kappa\tau|^2 \frac{1}{n}|s_{n-1}|^2 . \tag{4.3}$$

In this limit the cotangent state (3.16) approaches a coherent state with Poisson photon statistics and mean photon number $\langle n \rangle = |2\alpha/\beta\kappa\tau|^2$. Although this is essentially the same state as reached by an oscillator driven by a classical current,[9] we emphasize that during its evolution to steady state, it was crucial that the oscillator feels the presence of the trapping state $|N_1\rangle$. Hence it had to probe number states such that the condition $\kappa\tau \ll 1/\sqrt{n}$ is not fulfilled. Indeed, the oscillator would not even reach a pure state if $|N_1\rangle$ were a trapping state of even parity. This is a clear indication of the importance of its "granular nature" and of quantum dynamics at play.

Consider next the situation where the cotangent state is bound between the vacuum and a 3π trap, i.e., condition (4.2) is satisfied at $x = 3\pi/2$, but not at $\pi/2$. In this case, it is quite clear that the photon statistics of the cotangent state can become double peaked for appropriate values of β/α. Such a state is illustrated in Fig. 2. More complicated photon statistics, e.g., with multiple peaks, are possible if the state is confined in a phase-space region bound by a higher-order odd-π trapping state.

V. DYNAMICS

So far we have limited our discussion to the steady states asymptotically reached by the cavity mode. To determine the dynamical evolution of the field we now turn to an analysis of the eigenvalues of the discrete map

$$\rho_l = \mathcal{M}_0 \rho_{l-1} , \tag{5.1}$$

giving the reduced field density matrix after the passage of l atoms from its value after $l-1$ atoms. From Eqs. (2.1) and (3.1), the density-matrix element $\rho_{l;n,m} = \langle n|\rho_l|m \rangle$ is given by

$$\rho_{l;n,m} = \langle n|\mathcal{M}_0\rho_{l-1}|m \rangle$$

$$= \rho_{l-1;n,m}|\alpha|^2\cos(\sqrt{n+1}\kappa\tau)\cos(\sqrt{m+1}\kappa\tau) + \rho_{l-1;n+1,m+1}|\beta|^2\sin(\sqrt{n+1}\kappa\tau)\sin(\sqrt{m+1}\kappa\tau)$$

$$+ i\rho_{l-1;n+1,m}\alpha^*\beta\sin(\sqrt{n+1}\kappa\tau)\cos(\sqrt{m+1}\kappa\tau) - i\rho_{l-1;n,m+1}\alpha\beta^*\cos(\sqrt{n+1}\kappa\tau)\sin(\sqrt{m+1}\kappa\tau)$$

$$+ \rho_{l-1;n-1,m-1}|\alpha|^2\sin(\sqrt{n}\kappa\tau)\sin(\sqrt{m}\kappa\tau) + \rho_{l-1;n,m}|\beta|^2\cos(\sqrt{n}\kappa\tau)\cos(\sqrt{m}\kappa\tau)$$

$$+ i\rho_{l-1;n-1,m}\alpha\beta^*\sin(\sqrt{n}\kappa\tau)\cos(\sqrt{m}\kappa\tau) - i\rho_{l-1;n,m-1}\alpha^*\beta\cos(\sqrt{n}\kappa\tau)\sin(\sqrt{m}\kappa\tau) . \tag{5.2}$$

It is useful in the following to think of the matrix elements of ρ as defining a complex vector with $(N_u - N_d + 1)^2$ elements. The $(N_u - N_d + 1)^2$ complex eigenvalues Λ of the map (5.1) are given by

$$\mathcal{M}_0 - \Lambda 1 = 0 . \tag{5.3}$$

We reduce the dimensionality of the problem by exploiting the fact that any physically allowed field density matrix ρ must be Hermitian. If it is confined between the trapping states $|N_d\rangle$ and $|N_u\rangle$ it is fully defined by its $(N_u - N_d + 1)$ real diagonal elements and by $(N_u - N_d + 1)(N_u - N_d)/2$ complex off-diagonal elements, or equivalently by $(N_u - N_d + 1)^2$ real elements. We can thus organize the relevant elements of the density matrix ρ as a real "supervector" $\mathcal{R}$ with $(N_u - N_d + 1)^2$ elements

and whose evolution is given by the reduced real map $\mathcal{M}$

$$\mathcal{R}_l = \mathcal{M}\mathcal{R}_{l-1} \tag{5.4}$$

with $(N_u - N_d + 1)^2$ real eigenvalues. We use the condition $\text{Tr}\rho = 1$ to normalize the eigenvectors of $\mathcal{M}$.

Any physically allowed field density matrix is expressed as a linear combination of the eigenvectors r_μ of $\mathcal{M}$ as

$$\mathcal{R} = \sum_\mu c_\mu r_\mu . \tag{5.5}$$

After l iterations of the map (5.4), an initial density matrix described by the supervector $\mathcal{R}_0$ evolves to

$$\mathcal{R}_l = \sum_\mu (\lambda_\mu)^l c_\mu r_\mu , \tag{5.6}$$

where λ_μ is the real eigenvalue corresponding to the eigenvector κ_μ. The micromaser transients are governed by the eigenvectors κ_μ with $-1 \le \lambda_\mu \le 1$, while the fixed points are given by the eigenvectors with unit eigenvalue.

A few remarks are called for at this point. First, because of the conservation of the trace, it is obvious on physical grounds that the eigenvectors with nonunit eigenvalue must correspond to traceless density matrices, while those with $\lambda_\mu = 1$ must have unit trace when properly normalized. This is precisely the result found numerically. Second, it is in principle possible to have eigenvectors with eigenvalues $\lambda_\mu = -1$. Their existence leads to "period-2" oscillations of the quantum map (5.4). Finally, if more than one eigenvector has unit absolute eigenvalue $|\lambda_\mu| = 1$ an initial mixture ρ_0 with nonzero components on these two eigenvectors will always remain in a mixed state. Hence, from the numerical results of Sec. II, we expect only one eigenvector with unit eigenvalue in the case of a field bound between two trapping states of opposite parities.

We have numerically determined the eigenvectors and eigenvalues of the map (5.5) for field density matrices confined between the vacuum state $|0\rangle$ and the upper trapping state $|N_u\rangle$ up to $N_u = 18$. In each case, we have considered $|N_u\rangle$ to be a $q\pi$ trap $(N_u+1)^{1/2}\kappa\tau = q\pi$ with q an integer between 1 and 10. In the normal situation where there is no intervening trapping state between $|0\rangle$ and $|N_u\rangle$, we have found that the map has only one eigenvector with unit eigenvalue. This eigenvector is precisely the cotangent solution (3.14) for q odd, while it corresponds to a mixed state for q even in agreement with the results of Sec. III and of the Appendix. Our analysis also indicates that the other eigenvectors κ_μ tend to be grouped in two clusters, one with eigenvalues close to zero and the other with eigenvalues close to unity. The first group contributes to rapidly decaying transients, while the eigenvectors with eigenvalues close to unity lead to the slow exponential approach to steady state il-
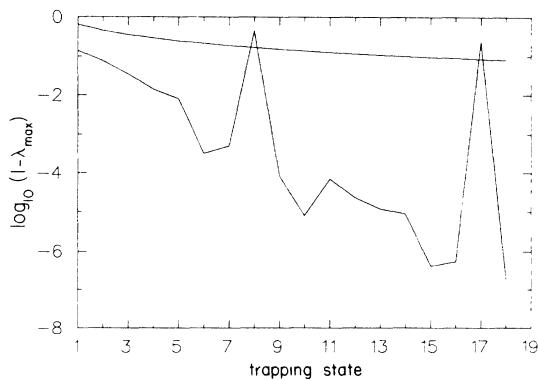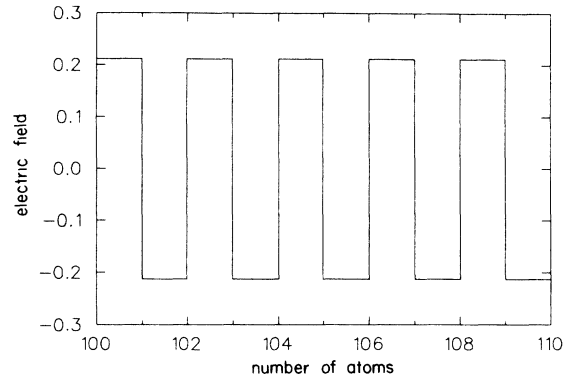

FIG. 8. Period-2 oscillations of a cavity field initially in a coherent state with mean photon number $\langle n \rangle = 1$, $|\alpha|^2 = 0.5$. The number state $|8\rangle$ is a 3π-trapping state, so that the number state $|1\rangle$ is a π trap.

lustrated in Figs. 1(a) and 2(b). Our numerical results show that the higher q, the closer to unity this last group of eigenvalues tends to be, as illustrated in Fig. 7. Also, for a given type of trapping, as the highest nonunit eigenvalue becomes closer to 1, the higher the trapping state, so that the approach to steady state requires an increasing large number of atoms to pass through the cavity. These trends are illustrated in Figs. 1(b) and 2(b) and indicate that it will take a very large number of atoms to prepare states resembling "macroscopic" superpositions. From a practical viewpoint, cavity losses will eventually become important, thereby limiting the degree of macroscopic separation that can experimentally be achieved.

In the case where there is an accidental trap between $|0\rangle$ and $|N_u\rangle$, we typically find two eigenvectors with unit eigenvalue, as well as traceless eigenvectors with eigenvalue -1. Although traceless, these eigenvectors have observable effects; they influence the off-diagonal elements of the field density matrix and hence e.g., the expectation value of the electric field. The eigenvalue -1 is also a signature of a period-2 dynamical behavior: the state of the cavity mode repeats each two atoms. Figure 8 shows such a situation where the field undergoes period-2 oscillations as successive atoms are injected inside the cavity.

VI. SUMMARY AND CONCLUSIONS

In this paper, we have shown that a lossless single-mode micromaser driven by a sequence of spin-$\frac{1}{2}$ particles can evolve to a new class of pure states of the electromagnetic field. Under appropriate conditions, these states can be sub-Poissonian or even number states, or resemble macroscopic superpositions. The experimental verification of these predictions requires overcoming the considerable experimental challenge of preparing all atoms in precisely the same coherent superposition. The phase fluctuations in the superposition (2.4) are presently being investigated both analytically and numerically following techniques similar to those described in Ref. 10.

FIG. 7. $\log_{10}(1-\lambda_{max})$ for increasing number states $|n\rangle$. Here λ_{max} is the largest eigenvalue of the map (5.4) less than unity. The smooth line is for $|n\rangle$ being a π trap, and the jagged line is for $|n\rangle$ being a 3π trap. The peaks in this second curve at $|n\rangle = |8\rangle$ and $|17\rangle$ correspond to the appearance of intervening π traps, i.e., they are such that $n+1 = 9q$, q integer.

A further obstacle, specially concerning the generation of macroscopic superpositions, is dissipation, as it is well known that macroscopic superpositions are very sensitive to damping.[11] However, the exceedingly high-Q ($Q \geq 10^{10}$) of micromaser cavities, which correspond to cavity damping times approaching a tenth of a second, provide an excellent starting point for potential experiments: even for "macroscopic superpositions" decaying several orders of magnitude faster than this rate, there might be a possibility of performing transient measurements over a reasonable time scale. Finally, when thinking of potential experiments we should keep in mind that although this paper treats explicitly the case of a micromaser, our considerations carry over to the more general situation of any harmonic oscillator driven by a quantum current of spin-$\frac{1}{2}$ particles.

Note added in proof. We have shown in the meantime that macroscopic superpositions can survive in the micromaser in steady state and in the presence of dissipation.[12]

ACKNOWLEDGMENTS

We have enjoyed numerous conversations with S. L. Braunstein, C. M. Savage, and E. M. Wright. This research is supported by Office of Naval Research (ONR) Contract No. N00014-88-K-0294 and by the Joint Services Optics Program. Computations were performed in part at the John von Neumann Computer Center.

APPENDIX

In this appendix, we impose that the states (3.14) and (3.15) satisfy the trapping condition (3.3) at the boundaries of the phase-space block under consideration. These boundary conditions are satisfied provided that the upper and lower trapping states $|N_u\rangle$ and $|N_d\rangle$ have opposite parities: specifically, the cotangent state (3.14) only satisfies the boundary conditions if $\sqrt{N_d+1}\kappa\tau=q\pi$, q

even and $\sqrt{N_u+1}\kappa\tau=p\pi$, p odd. The reverse is true for the tangent solution (3.15): in that case q must be odd and p even.

Consider first the down-trapping state $|N_d\rangle$, which satisfies

$$\sqrt{N_d}\kappa\tau=p\pi \ . \tag{A1}$$

For this state, conditions (3.8) and (3.9) become

$$s_{(N_d-1)}=\frac{i\beta\sin(\sqrt{N_d}\kappa\tau)}{\alpha'\exp(i\phi)-\alpha\cos(\sqrt{N_d}\kappa\tau)}s_{N_d}=0 \ , \tag{A2}$$

$$s_{(N_d-1)}=-i\frac{\beta'\exp(i\phi)-\beta\cos(\sqrt{N_d}\kappa\tau)}{\alpha\sin(\sqrt{N_d}\kappa\tau)}s_{N_d}=0 \ , \tag{A3}$$

Equation (A2) is automatically satisfied under the trapping condition (A1), and under this same condition Eq. (A3) only leads to normalizable states if

$$(\beta'/\beta)\exp(i\phi)=(-1)^q \ . \tag{A4}$$

For q even, this is fulfilled by the cotangent solution (3.12) only and for q odd by the tangent solution (3.13) only. Turning to the boundary conditions at the upper-trapping state $|N_u\rangle$, with

$$\sqrt{N_d}\kappa\tau=p\pi \tag{A5}$$

we find similarly

$$(\alpha'/\alpha)\exp(i\phi)=(-1)^p \ . \tag{A6}$$

For p even, this yields the tangent solution (3.13) and for p odd the cotangent state (3.12). Combining the results of the upper and lower trap boundary conditions proves that the upper and lower traps must have opposite parities. For q even and p odd, the solution is the cotangent state and for q odd and p even it is the tangent state. No pure state solution is possible in other situations.

[1]J. Mod. Opt. **34**, Special Issue (1987); J. Opt. Soc. Am. B **4**, Special Issue (1987).

[2]P. Filipowicz, J. Javanainen, and P. Meystre, J. Opt. Soc. Am. B **3**, 906 (1986).

[3]J. J. Slosser, P. Meystre, and S. L. Braunstein, Phys. Rev. Lett. **63**, 934 (1989).

[4]F. W. Cummings and A. K. Rajagopal, Phys. Rev. A **39**, 3414 (1989).

[5]D. Meschede, H. Walther, and G. Müller, Phys. Rev. Lett. **54**, 551 (1985).

[6]E. T. Jaynes and F. W. Cummings, Proc. IEEE **51**, 89 (1963).

[7]E. B. Davies, *Quantum Theory of Open Systems* (Academic, London, 1976); K. Krauss, *States, Effects and Operations:*

Fundamental Notions of Quantum Theory (Springer-Verlag, Berlin, 1983).

[8]See, e.g., W. H. Louisell, *Quantum Statistical Properties of Radiation* (Wiley, New York, 1973).

[9]R. J. Glauber, Phys. Rev. **131**, 2766 (1963).

[10]P. Meystre and J. J. Slosser, Opt. Commun. **70**, 103 (1989).

[11]A. O. Caldeira and A. J. Leggett, Phys. Rev. A **31**, 1059 (1985); for quantum optical situations, see, e.g., D. F. Walls and G. J. Milburn, Phys. Rev. A **31**, 2403 (1985); C. M. Savage and D. F. Walls, Phys. Rev. A **32**, 2316 (1985).

[12]J. J. Slosser, P. Meystre, and E. M. Wright, Opt. Lett. **15**, 233 (1990).